PHYSICAL REVIEW B **76**, 144103 (2007)

Nonlinear response theories and effective pair potentials

Simon Gravel and N. W. Ashcroft
Laboratory of Atomic and Solid-State Physics, Cornell University, Ithaca, New York 14850-2501, USA

(Received 20 March 2007; revised manuscript received 12 July 2007; published 4 October 2007)

We present a general method based on nonlinear response theory to obtain effective interactions between ions in an interacting electron gas, which can also be applied to other systems where an adiabatic separation of time scales is possible. Nonlinear contributions to the interatomic potential are expressed in terms of physically meaningful quantities, giving insight into the physical properties of the system. The method is applied to various test cases and is found to improve the standard linear and quadratic response approaches. It also reduces the discrepancies previously observed between perturbation theory and density functional theory results for proton-proton pair potentials in metallic environments.

DOI: 10.1103/PhysRevB.76.144103 PACS number(s): 62.50.+p, 34.20.Cf, 71.15.Mb, 71.45.Gm

I. INTRODUCTION AND BACKGROUND

Perturbation and response theories are ubiquitous in physics. Here we will discuss response theories as applied to many-component systems, where the degrees of freedom associated with one component can be traced out to yield, via an adiabatic separation of time scales, effective interactions between the remaining components. These effective interactions have had their share of success in describing simple metals,[1,2] metals with magnetic impurities [i.e., the Ruderman-Kittel-Kasuya-Yosida (RKKY) interaction[3]], or, in the classical domain, colloidal suspensions [e.g., the Derjaguin-Landau-Verwey-Overbeek (DLVO) interaction between charged colloidal particles[4,5] or the depletion interaction[6,7]]. Linear response in particular has been used extensively to obtain pair potentials; its simplicity makes it a very valuable qualitative tool, and in many contexts it also provides sufficient quantitative accuracy.

Higher-order contributions have been used less often, partly because calculational complexity increases rapidly with the order of perturbation considered. The first derivation of the static quadratic response function for the ground-state noninteracting electron gas originates with Lloyd and Sholl.[8] It was later rederived by Brovman, Kagan, *et al.*, who wrote a series of articles applying nonlinear perturbation to metallic systems (see, for example, Brovman, Kagan, and Kholas,[9] and references therein). A third derivation of the static response function was provided even later by Milchev and Pickenheim.[10] A derivation of the dynamical quadratic response function can also be found in Pitarke *et al.*[11] With the advent of density functional theory (DFT) and modern computers, response theory has lost some of its quantitative appeal, but as noted it is still being used for a qualitative understanding of general trends in metals.[11–13]

Dynamic compression experiments have achieved metallization of hydrogen at high temperature,[14] and there is an expectation that low-temperature metallization might also be achieved in the relatively near future.[15] Hydrogen has always been difficult to treat by perturbation approaches because the interaction of a proton with the electron gas is not weakened by a repulsive core, as is the case for many elements.[16] It is not even obvious that a perturbation approach converges. At high pressures, though, the enhanced kinetic energy of the electron gas in hydrogen leads to a better convergence of response theory. Response-based pair potentials were in fact used to describe with some success the pressure dependence of the vibron in the hydrogen solid.[17] On the other hand, the application of standard DFT methods to hydrogen at very high densities is challenging because of the strongly inhomogeneous, cusplike electronic density surrounding the proton and the possible failure of pseudopotentials designed for a different density range. The pair potentials obtained from quadratic perturbation theory for dense hydrogen exhibit discrepancies when compared with *ab initio* DFT results[18] for Wigner-Seitz radii as low as 1.3. The Wigner-Seitz radius r_s is related to the unperturbed electronic density ρ_0 by $r_s a_0 = [3/(4\pi\rho_0)]^{1/3}$, where $a_0 = \hbar^2/m_e e^2$ is the Bohr radius.

In order to use the perturbation method as a reliable, analytic alternative approach to DFT in this density range, higher-order terms are needed. Going beyond quadratic response using conventional methods is a substantially more difficult task. Accordingly, we derive a simple identity that allows us to obtain effective pair potentials beyond quadratic response, which amounts to carrying out a partial sum of perturbation terms. The result is not only very intuitive, expressing the pair potential in terms of physically meaningful expressions, but also very general, since it applies in any dimension and for both classical and quantum systems. Moreover, it does not require explicit knowledge of the nonlinear response functions. It should be noted that if nonlinear effects are to be fully taken into account, many-body interactions should also be included, either directly or through effective-medium approaches.[33] This article focuses on obtaining pair potentials that can be used as a starting point for either approach.

In Sec. II, we outline the response theory formalism and derive the simplest version of our result, Eq. (12). In Sec. III (and Appendix A) a generalization is derived that applies to homogeneous, interacting systems. The intuitive nature of this result permits us to explain part of the discrepancies observed between the results of Nagao *et al.*[17] and Bonev and Ashcroft[18] and to improve upon quadratic response. In Sec. IV we apply our results to obtain pair potentials in various systems, including metallic hydrogen. Generalizations to many-center interactions and magnetic perturbations are discussed in Appendix B.

II. EFFECTIVE INTERACTIONS AND RESPONSE THEORY

We start with a canonical system composed of a mixture of at least two different types of particles, in contact with a heat bath establishing a temperature T. The ground-state properties of the system can be studied from the limit $T \to 0$.

The particles will be divided in two subsets, labeled L (for light, typically electrons) and M (for massive, typically ions). It is assumed that all L particles are identical. On the other hand, the set M can contain various types of particles. The time scales associated with the L particles will be assumed to be much shorter than those associated with the M particles, allowing the use of an adiabatic separation of time scales. In real systems, this separation is not exact. The assumption of exact separation of time scales, which will be made throughout this article, is referred to as the adiabatic or Born-Oppenheimer approximation. We will not discuss the accuracy of this approximation here and refer the reader to the existing literature (see, e.g., Ziman[19]).

The adiabatic approximation allows the treatment of the degrees of freedom associated with the light particles L in an average way, leading to a much simpler *effective* Hamiltonian for the remaining M particles.

The Hamiltonian of the initial system has the form

$$H = \sum_i \frac{\mathbf{p}_i^2}{2m} + \sum_j \frac{\mathbf{P}_j^2}{2M_j} + V^M(\{\mathbf{R}\}) + V^L(\{\mathbf{r}\}) + V^{LM}(\{\mathbf{r}\},\{\mathbf{R}\}). \tag{1}$$

The notation $\{\mathbf{r}\}$ designates the set of all coordinates $\{\mathbf{r}_i\}_{i=1,\ldots,N_L}$, and $\mathbf{p}_i$, $\mathbf{r}_i$, and m are the momenta, positions, and mass of L particles, while $\mathbf{P}_i$, $\mathbf{R}_i$, and M_i are the corresponding quantities for M particles. We imagine the system to be confined to a macroscopic volume Ω.

In many relevant physical systems the interactions between the particles are largely pairwise. An important example of such a system is a metal, where the L particles could be the valence electrons and the M particles the ionic cores. For pairwise systems we can write

$$V^L(\{\mathbf{r}\}) = \sum_i \phi_L^{(1)}(\mathbf{r}_i) + \sum_{i\neq j} v^L(\mathbf{r}_i,\mathbf{r}_j),$$

$$V^M(\{\mathbf{R}\}) = \sum_i \phi_M^{(1)}(\mathbf{R}_i) + \sum_{i\neq j} v_{ij}^M(\mathbf{R}_i,\mathbf{R}_j),$$

$$V^{LM}(\{\mathbf{r}\},\{\mathbf{R}\}) = \sum_{ij} v_j^{LM}(\mathbf{r}_i,\mathbf{R}_j), \tag{2}$$

where $\phi_L^{(1)}$ and $\phi_M^{(1)}$ denote external, one-particle potentials, v^L is the pair potential between L particles, v_{ij}^M is the pair potential between M particles i and j, and v_j^{LM} is the pair potential between the M particle j and the L particles. In the case of long-range, Coulombic interactions, care should be taken in the definition of the pair potentials to ensure that both the unperturbed and the perturbing systems are thermodynamically well defined.[20]

We will restrict our attention to such pairwise systems, even though our main results require only the slightly weaker assumptions that we can write the interaction between L and M particles as

$$V^{LM}(\{\mathbf{r}\},\{\mathbf{R}\}) = \sum_i V_1^{LM}(\mathbf{r}_i,\{\mathbf{R}\}).$$

This is to say that the joint effect of all M particles, if they were held fixed, would amount to an additional one-body potential for the L particles.

A. Effective interactions and the adiabatic separation of time scales

As mentioned, we want to find an *effective* Hamiltonian for the M particles by tracing out the degrees of freedom associated with the L particles. Since volume (Ω) and temperature (T) are specified, we begin with the relevant Helmholtz free energy F,

$$F = -kT \ln \mathrm{Tr}_{\{LM\}} e^{-\beta H}. \tag{3}$$

We then trace over the degrees of freedom associated with L at fixed configuration of M, assuming an adiabatic separation of time scales,

$$F = -kT \ln(\mathrm{Tr}_M e^{-\beta(T^M+V^M)} \mathrm{Tr}_{L(M)} e^{-\beta(T^L+V^L+V^{LM})}),$$

where $\mathrm{Tr}_{L(M)}$ means the trace over states of particles of type L for a fixed configuration of particles M, and $T^{\{L,M\}}$ is the kinetic energy associated with the L and M particles, respectively. The free energy of system L for a fixed configuration of M is simply

$$F_L(\{\mathbf{R}\},T) = -kT \ln(\mathrm{Tr}_{L(M)} e^{-\beta(T^L+V^L+V^{LM})}). \tag{4}$$

The total free energy can then be written as

$$F = -kT \ln \mathrm{Tr}_M e^{-\beta H_M^{eff}}, \tag{5}$$

where the effective Hamiltonian has the form

$$H^{eff} = \sum_j \frac{\mathbf{P}_j^2}{2M_j} + V^M(\{\mathbf{R}\}) + V^{eff}(\{\mathbf{R}\})$$

and $V^{eff}(\{\mathbf{R}\}) = F_L(\{\mathbf{R}\},T)$ is the desired effective interaction between particles of type M. It is clearly state dependent, since it depends on temperature. It also depends on the volume Ω and on the properties of the L particles, including their mass, their number, and the form of their interactions. Note that even if the initial Hamiltonian contains only pairwise interactions, the *effective* Hamiltonian will typically contain many-center interactions as well as volume-dependent but structure-independent terms. Here we will focus on the determination of pair interactions.

In order to obtain the effective interaction we need to calculate the free energy (4) of system L while the M particles are held fixed. To do this we treat the potential $V_1^{LM}(\mathbf{r},\{\mathbf{R}\})$ as an external one-body perturbation to the system composed of particles of type L. In the following $V_1^{LM}(\mathbf{r},\{\mathbf{R}\})$ will therefore be simply written as $V_{ext}(\mathbf{r})$, keeping in mind the dependence of V_{ext} on the $\mathbf{R}_i$. We then proceed to a functional expansion of the free energy in orders of $V_{ext}(\mathbf{k})$,[20]

$$V_{ext}(\mathbf{k}) = \int_\Omega d\mathbf{r}\, e^{-i\mathbf{k}\cdot\mathbf{r}} V_{ext}(\mathbf{r}).$$

B. Response theory, and the coupling-constant integration method

The change in density induced in a system by a perturbing external potential $V_{ext}(\mathbf{k})$ takes the form

$$\delta\rho(\mathbf{k},T) = \rho(\mathbf{k},T) - \rho^{(0)}(\mathbf{k},T) = \sum_{\mathbf{k}'} \chi^{(1)}(-\mathbf{k},\mathbf{k}',T) V_{ext}(\mathbf{k}') + \frac{1}{\Omega}\sum_{\mathbf{k}',\mathbf{k}''} \chi^{(2)}(-\mathbf{k},\mathbf{k}',\mathbf{k}'',T) V_{ext}(\mathbf{k}') V_{ext}(\mathbf{k}'') + \cdots. \tag{6}$$

The functions $\chi^{(n)}$ are, by definition, the response functions of the unperturbed system (which at this point is not necessarily uniform) and carry all the information about this system, including temperature. We have assumed a large but finite volume Ω and a dense but discrete distribution of wave vectors $\mathbf{k}$, since our main interest is the electron gas. Continuous systems can be recovered using the usual prescription[20] [in three dimensions, it reads $1/\Omega\Sigma_{\mathbf{k}} \rightarrow \int d\mathbf{k}/(2\pi)^3$]. Even though the response functions depend on temperature, the methods we present here do not involve this temperature dependence explicitly. In order to simplify the notation, we will not explicitly keep track of the temperature in the following. Unless otherwise specified, $\chi^{(1)}(\mathbf{k},\mathbf{k}')$ will simply stand for $\chi^{(1)}(\mathbf{k},\mathbf{k}',T)$, etc.

Equation (6) can be used together with the coupling-constant integration method[21,22] to obtain the variation in the Helmholtz free energy arising from the perturbation V_{ext}: namely,

$$\Delta F = \int_0^1 d\lambda \langle V_{ext}\rangle_\lambda, \tag{7}$$

where $\langle\cdot\rangle_\lambda$ is the statistical average with respect to the states of the Hamiltonian H_λ^{ext}, which is obtained by replacing V_{ext} by λV_{ext} in H^{ext}. In the thermodynamic integration scheme,[23] the integrand in Eq. (7) is determined by numerical simulation. In the perturbation approach, it is instead expanded in powers of the external perturbation, yielding

$$\begin{aligned}\Delta F &= \frac{1}{\Omega}\sum_{\mathbf{k},n} \frac{\rho^{(n)}(\mathbf{k}) V_{ext}(-\mathbf{k})}{n+1} \\ &= \sum_{n=0}^{\infty} \frac{1}{(n+1)\Omega^n} \sum_{\mathbf{k}_1,\ldots,\mathbf{k}_{n+1}} \chi^{(n)}(\mathbf{k}_1,\ldots,\mathbf{k}_{n+1}) \\ &\quad\times V_{ext}(\mathbf{k}_1)\cdots V_{ext}(\mathbf{k}_{n+1}),\end{aligned} \tag{8}$$

where $\rho^{(n)}$ is the part of Eq. (6) that is of order n in V_{ext}. The "zeroth-order" response function is related to the density of the unperturbed system, $\chi^{(0)}(\mathbf{k}) = \rho^{(0)}(-\mathbf{k})/\Omega$.

Note that terms of nth order in the external potential in expression (6) yield terms of order $n+1$ in Eq. (8). In the following, "nth-order response" refers to terms of order n in Eq. (6), unless otherwise specified.

In order to study pair potentials, let us now assume that the perturbation originates with *two* external sources, located at positions $\mathbf{R}_a$ and $\mathbf{R}_b$, so that

$$V_{ext}(\mathbf{k}) = V_a(\mathbf{k}) e^{i\mathbf{k}\cdot\mathbf{R}_a} + V_b(\mathbf{k}) e^{i\mathbf{k}\cdot\mathbf{R}_b}.$$

The free energy now depends on $\mathbf{R}_a$ and $\mathbf{R}_b$ (and would depend only on $\mathbf{R}_a - \mathbf{R}_b$ if we had restricted ourselves to initially homogeneous systems). This yields an induced effective pair potential $\phi^i(\mathbf{R}_a,\mathbf{R}_b)$ between the two sources, defined as the sum of all terms in Eq. (8) that depend on both V_a and V_b. Here the standard approach is to keep only terms up to a given order in V_{ext}. Linear response yields the *induced* pair potential

$$\phi^i_{lin}(\mathbf{R}_a,\mathbf{R}_b) = \frac{1}{\Omega}\sum_{\mathbf{k},\mathbf{k}'} \chi^{(1)}(\mathbf{k},\mathbf{k}') V_a(\mathbf{k}) V_b(\mathbf{k}') e^{i(\mathbf{k}\cdot\mathbf{R}_a + \mathbf{k}'\cdot\mathbf{R}_b)}. \tag{9}$$

In order to emphasize the role of the coupling-constant integration and to hint at an upcoming result [Eq. (12)], this can be written as

$$\begin{aligned}\phi^i_{lin}(\mathbf{R}_a,\mathbf{R}_b) &= \frac{1}{\Omega}\sum_{\mathbf{k}} [V_a(\mathbf{k})\delta\rho_b^{lin}(-\mathbf{k},\mathbf{R}_b) e^{i\mathbf{k}\cdot\mathbf{R}_a} + V_b(\mathbf{k})\delta\rho_a^{lin}(-\mathbf{k},\mathbf{R}_a) e^{i\mathbf{k}\cdot\mathbf{R}_b}] \\ &\quad - \frac{1}{\Omega}\sum_{\mathbf{k}_1,\mathbf{k}_2} \chi^{(1)}(\mathbf{k}_1,\mathbf{k}_2) V_a(\mathbf{k}_1) V_b(\mathbf{k}_2) e^{i(\mathbf{k}_1\cdot\mathbf{R}_a + \mathbf{k}_2\cdot\mathbf{R}_b)},\end{aligned} \tag{10}$$

where $\delta\rho_i^{lin}(-\mathbf{k},\mathbf{R}_i)$ is the density induced, at linear order, by particle i located at position $\mathbf{R}_i$.

The first two terms in this expression correspond to the Coulombic energy of the system at the level of linear response. The third term, which arises from the coupling-constant integration, incorporates the variation in kinetic energy and entropy caused by the perturbation.

Instead of keeping terms linear in V_{ext}, we can choose to keep all terms that are linear in V_a, for all orders in V_b. In this case we find, using Eq. (6), that the pair potential can be written as

$$\phi^i(\mathbf{R}_a,\mathbf{R}_b) \simeq \phi^i_{SPb}(\mathbf{R}_a,\mathbf{R}_b) = \frac{1}{\Omega}\sum_{\mathbf{k}} V_a(\mathbf{k})\,\delta\rho_b(-\mathbf{k},\mathbf{R}_b)e^{i\mathbf{k}\cdot\mathbf{R}_a}. \tag{11}$$

Here, $\delta\rho_b(\mathbf{k},\mathbf{R}_b)$ is the total density that would be induced if the perturbation potential was caused by source b alone—i.e., $V_{ext}(\mathbf{k})=V_b(\mathbf{k})e^{i\mathbf{k}\cdot\mathbf{R}_b}$. Notice that the terms arising from the interaction between $\delta\rho_a$ and V_b and the change in kinetic energy and entropy arising from the perturbation (taken into account by the coupling-constant integration) cancel each other out exactly in this case. One can also obtain a different estimate to the potential by inverting the roles of a and b in the previous discussion, leading to ϕ^i_{SPa}.

This asymmetric approach will be referred to as the successive perturbation method (SPM). Indeed, one interpretation of this result is that instead of perturbing the initial system with a and b simultaneously, we initially add only b, determine the properties of the intermediate system, and then, subsequently, add particle a. Since our pair potentials result from the calculation of a free energy, the Gibbs-Bogoliubov inequality applies and Eq. (11) is related to a rigorous bound on the pair potential: namely,

$$\phi^i(\mathbf{R}_a,\mathbf{R}_b) \le \phi^i_{SPb}(\mathbf{R}_a,\mathbf{R}_b) + \langle V_a\rangle_0 - \Delta F_a,$$

where $\langle V_a\rangle_0$ is the statistical average of the operator $V_a(\mathbf{k})e^{i\mathbf{k}\cdot\mathbf{R}_a}$ with respect to states of the initial, unperturbed system, and ΔF_a is the change in free energy induced by adding a to the unperturbed system, which can be obtained by setting $V_b=0$ in Eq. (8).

Equation (11) is the first term in the expansion of the energy if b is treated exactly and a is treated as a perturbation. Note that higher-order terms in the expansion would simply involve higher-order functional derivatives of the free energy of the intermediate system including b, which are related to density-density correlation functions of that system.

The SPM is especially useful if V_a is weak and V_b is strong,[24] but is not as useful when both sources of perturbation are strong and require nonlinear treatment. On the other hand, we can easily obtain from this relation another expression for the induced pair potential that incorporates all contributions that are linear in *either* source. This expression therefore includes all contributions to the pair potential up to cubic order in V_a and V_b. It reads

$$\phi^i_{SSP}(\mathbf{R}_a,\mathbf{R}_b) = \frac{1}{\Omega}\sum_{\mathbf{k}}\left[V_a(\mathbf{k})\,\delta\rho_b(-\mathbf{k},\mathbf{R}_b)e^{i\mathbf{k}\cdot\mathbf{R}_a} + V_b(\mathbf{k})\,\delta\rho_a(-\mathbf{k},\mathbf{R}_a)e^{i\mathbf{k}\cdot\mathbf{R}_b}\right] - \frac{1}{\Omega}\sum_{\mathbf{k}_1,\mathbf{k}_2}\chi^{(1)}(\mathbf{k}_1,\mathbf{k}_2)V_a(\mathbf{k}_1)V_b(\mathbf{k}_2)e^{i(\mathbf{k}_1\cdot\mathbf{R}_a+\mathbf{k}_2\cdot\mathbf{R}_b)}. \tag{12}$$

This result, which emerges from what we will refer to as the symmetrized successive perturbation method (SSPM), can also be seen to be a natural generalization of linear response (10). Equation (12) is our main result for noninteracting systems. It also applies to interacting systems, but in that case it can be improved upon. We will do this in Sec. III.

Equation (12), despite its simplicity, has many interesting features:

(a) It is very general; it can be used in any dimension, for classical and quantum, homogeneous and inhomogeneous, noninteracting and interacting systems (although, as mentioned, it can be improved for interacting systems; see Sec. III). (b) It is intuitive: the first two terms are the interaction of the potential energy associated with each perturbation with the density induced by the other. The last term, which is equal to the negative of the linear response potential, accounts for the change in kinetic energy and entropy of the perturbed system and the contributions to the density that are not additive in V_a and V_b. (c) It includes all contributing terms up to quadratic response [yielding cubic terms in Eq. (8)], plus 8 out of 14 contributing terms of cubic response: it includes more terms than quadratic response. (d) It does not require the explicit knowledge of the second-order response function, but only that of the linear response function of the initial, unperturbed system. (e) It expresses the pair potentials in terms of quantities that are simple, symmetric, and can in principle be measured. Finally (f), since it takes the effect of a single, isolated perturbation as an external input, Eq. (12) allows us to treat the effect of stronger, localized perturbations which are often difficult to treat with purely perturbative methods.

We use this result in two test cases in Sec. IV. The first example is the effective interaction between particles perturbing, via δ-function potentials, a noninteracting quantum one-dimensional electron gas. The second is a version of the classical Asakura-Oosawa model[6,7] of the depletion interaction, with finite square wells replacing hard-sphere potentials. We then apply it to the more realistic calculation of the pair potential between protons in a metallic environment.

Before we do this, we use the intuitive form of Eq. (12) to suggest the existence of a higher-order correction that applies to interacting systems, which will be derived in Appendix A.

III. CORRECTIONS SPECIFIC TO INTERACTING SYSTEMS

As mentioned, Eq. (12) is valid for the interacting electron gas as well as for the noninteracting one: the interactions simply modify the forms of the $\chi^{(n)}$. But upon further inspection of this equation, one might wonder about the absence of coupling between the induced densities themselves. The part of this interaction that is linear in V_a or V_b is included in Eq. (12), but the part that is nonlinear in both V_a and V_b is not. It turns out that some of these contributions can also be expressed intuitively in terms of $\delta\rho_a$ and $\delta\rho_b$.

For *homogeneous* interacting systems we obtain, by summing up higher-order terms that correspond to reducible diagrams (see Appendix A), an extra term of the form

$$\phi_{red}(\mathbf{R}_{ab}) = \frac{1}{\Omega}\sum_{\mathbf{k}} \delta\rho_a^{NL}(\mathbf{k})\tilde{v}(k)\,\delta\rho_b^{NL}(-\mathbf{k})e^{i\mathbf{k}\cdot\mathbf{R}_{ab}}, \tag{13}$$

where $\mathbf{R}_{ab}$ is the distance between a and b, $\delta\rho_a^{NL}=\delta\rho_a-\delta\rho_a^{(1)}$, and $\tilde{v}$ is the effective interaction between the induced densities. It reads

$$\tilde{v}(k) = \epsilon(k)c_0^{(1)}(k), \tag{14}$$

where

$$\epsilon(k) = 1 - c_0^{(1)}(k)\chi_0(k)$$

involves the *noninteracting* response function $\chi_0^{(1)}$. In classical statistical mechanics $c_0^{(1)}(k)$ is the Ornstein-Zernike function for the unperturbed system, multiplied by k_BT. In the case of quantum mechanical particles of charge e, we have[20]

$$c_0^{(1)}(k) = v_c(k) + \mu_1(k),$$

where $v_c(k)=4\pi e^2/k^2$ is the Coulomb interaction and μ_1 is the first functional derivative with respect to density of the exchange-correlation potential. It is related to the local-field correction G by $\mu_1(k)=-G(k)v_c(k)$.

With some reorganization, we can now write the total induced pair potential in a remarkably simple form: namely,

$$\phi_{SSP}^{i}(\mathbf{k}) = \epsilon(k)[V_a(\mathbf{k})\,\delta\rho_b(-\mathbf{k}) + \delta\rho_a(\mathbf{k})V_b(-\mathbf{k}) + \delta\rho_a(\mathbf{k})c_0^{(1)}(k)\,\delta\rho_b(\mathbf{k}) - V_a(\mathbf{k})\chi_0^{(1)}(k)V_b(-\mathbf{k})]. \tag{15}$$

In real space,

$$\phi^{i}(\mathbf{R}_{ab}) = \frac{1}{\Omega}\sum_{\mathbf{k}} \phi^{i}(\mathbf{k})e^{i\mathbf{k}\cdot\mathbf{R}_{ab}}.$$

This result brings up an important point. The energy associated with the interaction between potential V_b and the nth-order contribution to the density induced by a, which we write as $\delta\rho_a^{(n)}$, arises at order $n+1$ in the energy expansion. On the other hand, the "electron-electron" interaction between $\delta\rho_a^{(n)}$ and $\delta\rho_b^{(n)}$ appears only at order $2n$ in the energy. Except for the special case of linear response, the electron-electron interaction terms originate with a higher order in response than the corresponding electron-perturbation terms. Therefore termination of the series (8) at any order beyond linear response will typically result in pair potentials that are overly attractive.

Indeed, if we compare the effective pair potentials for hydrogen atoms in jellium obtained from quadratic response[17] to those obtained from *ab initio* methods,[18] we observe exactly such a discrepancy. We calculate in Sec. IV C the lowest-order contribution arising from Eq. (13) and find that it indeed improves the agreement between *ab initio* methods and response theory.

We finally draw the reader's attention to the similarity (for protons in an electron gas) between the *ab initio* equation (15) and the variational Heitler-London evaluation of the isolated hydrogen molecule energy. This will be further discussed in Sec. IV C.

IV. EXAMPLES OF APPLICATIONS

A. Delta functions in a noninteracting electron gas

As a simple instructive example, we first consider a one-dimensional non-interacting electron gas of unperturbed linear density ρ_0 confined to a large length L, with periodic boundary conditions. The external perturbations have the form

$$V_\alpha(r) = \frac{\hbar^2 u}{2m}\delta(r) \quad (\alpha = a,b).$$

From Eq. (12) we obtain immediately

$$\phi_{SSP}(R_{ab}) \simeq \frac{\hbar^2 u}{2m}[2\,\delta\rho_a(R_{ab}) - \delta\rho^{lin}(R_{ab})]. \tag{16}$$

Here,

$$\delta\rho^{lin}(r) = \frac{\hbar^2 u}{2m}\sum_k \chi^{(1)}(k,-k)e^{ikr} \tag{17}$$

and $\chi^{(1)}$ is the linear response function of the one-dimensional non-interacting electron gas[3,25]:

$$\chi^{(1)}(k_1,k_2) = \frac{2m}{\hbar^2\pi k_1}\ln\left|\frac{k_1+2k_F}{k_1-2k_F}\right|\delta_{k_1,-k_2}.$$

The Fermi wave number k_F is related to the unperturbed linear density by $k_F=\pi\rho_0$.

Converting the sum into an integral, we find (see Kittel[3] and also Yafet[25] and Giuliani *et al.*[26])

$$\delta\rho^{lin}(r) = \frac{u}{\pi}\mathrm{Si}(2k_F r) - \frac{u}{2}, \tag{18}$$

where Si is the sine integral function.[27] The nonlinear induced density $\delta\rho_a(r)$ can also be calculated exactly as the sum of the bound and scattering state density: namely,

$$\delta\rho_a = \delta\rho_{bound} + \delta\rho_s,$$

with

$$\delta\rho_{bound}(r) = -\Theta(-u)ue^{u|r|} = \begin{cases} -ue^{u|r|} & \text{if } u<0, \\ 0 & \text{otherwise.}\end{cases} \tag{19}$$

Here Θ is the Heaviside step function.

The scattering state density is, in the limit of large L,[26]

$$\delta\rho_s(r) = \frac{2}{\pi}\int_0^{k_F} dk\left(\frac{2uk\sin(2k|r|)}{4k^2+u^2} - \frac{u^2\cos(2k|r|)}{4k^2+u^2}\right). \tag{20}$$

Factors of 2 are included for spin degeneracy. This integral can be evaluated in terms of the exponential integral E_1 using, for example, relations 5.1.41 and 5.1.42 from Abramowitz and Stegun.[27] We find

$$\delta\rho_s(r) = \frac{e^{u|r|}u}{\pi}\{\mathrm{Im}[\mathrm{E}_1((u+2ik_f)|r|)] + \pi\Theta(-u)\}. \tag{21}$$

The total density induced by a single δ-function potential in a noninteracting electron gas therefore takes the very simple form

$$\delta\rho_a(r) = \frac{ue^{u|r|}}{\pi}\,\mathrm{Im}\{\mathrm{E}_1((u+2ik_f)|r|)\}. \tag{22}$$

Note that for $k_f \to 0$ we find that $\delta\rho = \delta\rho_{bound}$, as expected. The appearance of a bound state at $u=0$ corresponds to the branch cut of E_1 along the negative real axis.

If we use Eqs. (18) and (22) in Eq. (16), we find an expression for the pair potential as a function of R_{ab} which reads

$$\phi_{SSP}(R_{ab}) = \frac{\hbar^2u^2}{\pi m}e^{uR_{ab}}\{\mathrm{Im}[\mathrm{E}_1((u+2ik_f)R_{ab})]\} - \frac{\hbar^2u^2}{2\pi m}\left(\mathrm{Si}(2k_F R_{ab}) - \frac{\pi}{2}\right). \tag{23}$$

Alternatively, the *exact* pair potential can be calculated by solving the Schrödinger's equation directly for different values of R_{ab}. The result is expressed as a sum over the eigenvalues of the Hamiltonian, which are obtained by numerically solving a set of transcendental equations.

We compare in Fig. 1 these numerical pair potentials with the analytical ones obtained from the SPM and SSPM [Eq. (23)], and those obtained from linear response, for various interaction strengths, including attractive and repulsive cases. We observe that the SSPM improves upon linear response and the SPM, especially quantitatively, at low u, but also qualitatively (at higher u).

As a side remark, notice that the system has no bound state for $u>0$, one even bound state for $u<0$, and one extra odd bound state when $R_{ab}u < -2$. It has been suggested[28] that the appearance of a bound state might cause the failure of response theory, since such states are qualitatively different from the initial, unperturbed free-electron system. We see that this is not the case in this particular example and that the pair potentials can be accurately described by response theory despite the presence of a bound state. This is consistent with the observation that no discontinuity in the density of charge occurs upon the formation of a localized, bound state (see, e.g., Galindo *et al.*[29]).

B. Classical depletion interaction

The depletion interaction (or entropic attraction) plays a major role in classical colloidal systems, where it is used to tune the interaction between colloidal particles immersed in a solvent. The addition of polymers to the solvent indeed causes an effective attraction between the colloidal particles which can be adjusted by modifying the polymer concentration.

The Asakura-Oosawa model[6,7] describes this effect by representing colloidal particles as hard spheres of radius D and (folded) polymers as hard spheres of radius δ. The interactions between the polymers are neglected. The polymers are therefore treated as an ideal gas which is excluded from spheres of radius $D+\delta$ surrounding each colloid. Here we will replace the hard-sphere potential with a finite repulsion of magnitude V_0. Within this model the effective attractive potential between the colloids can be calculated exactly and compared to the response theory results, providing a useful benchmark for perturbative approaches in the classical regime.

Suppose we have only two colloidal particles (at positions $\mathbf{R}_{a,b}$) in a bath of polymers of unperturbed density $\rho_0 = N/\Omega$. Since the polymers are taken not to interact, their density is given by

$$\rho(\mathbf{r}) = \frac{Ne^{-\beta V_e(\mathbf{r})}}{\int_\Omega d\mathbf{r}'\, e^{-\beta V_e(\mathbf{r}')}}, \tag{24}$$

where $V_e(\mathbf{r}) = V_a(\mathbf{r}) + V_b(\mathbf{r})$ is the total potential and

$$V_{a,b} = \begin{cases} V_0 & \text{if } |\mathbf{r}-\mathbf{R}_{a,b}| < D+\delta, \\ 0 & \text{otherwise.}\end{cases}$$

Since $V_e(\mathbf{r})$ is zero except within a bounded region, $\rho(\mathbf{r})$ simplifies, in the thermodynamic limit, to

$$\rho(\mathbf{r}) = \rho_0 e^{-\beta V_e(\mathbf{r})}. \tag{25}$$

Now we can use the coupling-constant integration method to obtain the Helmholtz free energy:

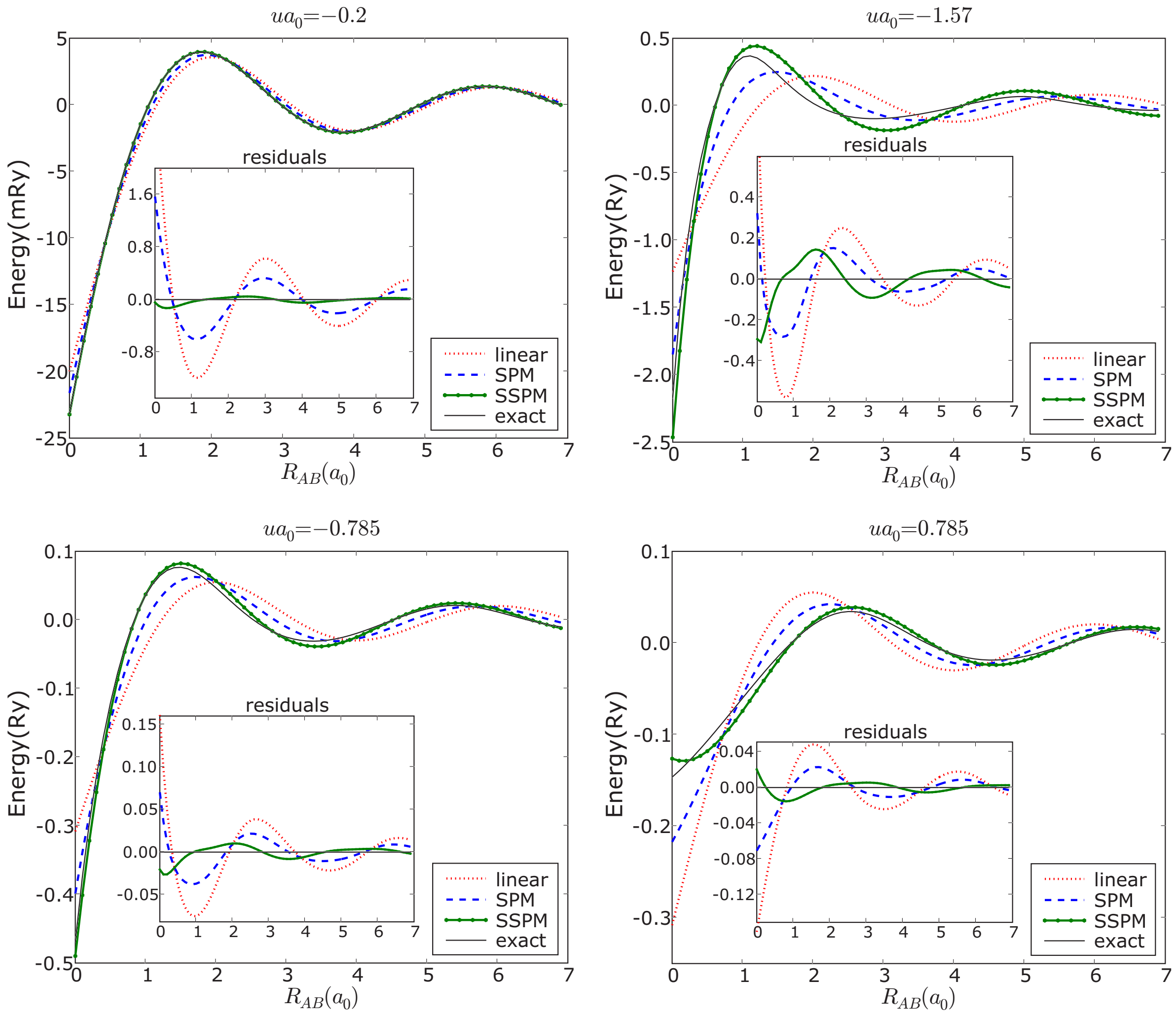

FIG. 1. (Color online) Pair potentials for δ-function potentials in one-dimensional noninteracting electron gas: exact, linear response, and the SPM and SSPM results. The Fermi wave vector is set to k_f=0.785/a_0. The residuals (difference between estimated and exact pair potentials) are shown in the inset. Note the difference in behavior of the SSPM near the origin between attractive (first three figures) and repulsive (last figure) δ-function potentials.

$$
\begin{aligned}
F - F_0 &= \int_0^1 d\lambda \int d\mathbf{r} V_{ext}(\mathbf{r})\rho_\lambda(\mathbf{r}) \\
&= - A_o(\mathbf{R}_a,\mathbf{R}_b)\frac{\rho_0}{\beta}(e^{-2\beta V_0} - 1) \\
&\quad - A_r(\mathbf{R}_a,\mathbf{R}_b)\frac{\rho_0}{\beta}(e^{-\beta V_0} - 1),
\end{aligned}
\tag{26}
$$

where A_o is the overlap volume between the two spheres of radius $D+\delta$ centered at $\mathbf{R}_{a,b}$, and $A_r = 8\pi(D+\delta)^3/3 - 2A_o$ is the nonoverlapping volume of the spheres. All the $\mathbf{R}_{a,b}$ dependence is contained in $A_o(\mathbf{R}_a,\mathbf{R}_b) = A_o(\mathbf{R}_a - \mathbf{R}_b)$. Accordingly we write the pair potential as

$$\phi^i(\mathbf{R}_a - \mathbf{R}_b, V_0) = -\frac{\rho_0 A_0(\mathbf{R}_a - \mathbf{R}_b)}{\beta}(e^{-\beta V_0} - 1)^2. \tag{27}$$

Notice the obvious limit $V_0 \to \infty$, yielding the familiar Asakura-Oosawa result,[6,7]

$$\phi^i(\mathbf{R}_a - \mathbf{R}_b, \infty) = -\frac{\rho_0 A_0(\mathbf{R}_a - \mathbf{R}_b)}{\beta}. \tag{28}$$

This problem can also be treated at various orders of response theory, using, e.g., $\chi^{(1)}(\mathbf{k},\mathbf{k}') = -\beta\rho_0\delta_{\mathbf{k},-\mathbf{k}'}$. The general form for the pair potential, which can be obtained by carrying the perturbation to any order, can be expressed as

$$\phi_n^i(\mathbf{R}_a - \mathbf{R}_b, V_0) = -f(\beta V_0)\frac{\rho_0 A_0(\mathbf{R}_a - \mathbf{R}_b)}{\beta}.$$

Only the position-independent function f is modified in the various approximations. The exact (nonperturbative) form for the function f is

$$f(x) = (e^{-x} - 1)^2.$$

We evaluate the performance of the various orders in response and of the SPM and SSPM by comparing the estimates obtained from each method to the exact result for $f(x)$. Since we know the exact result analytically, we can obtain

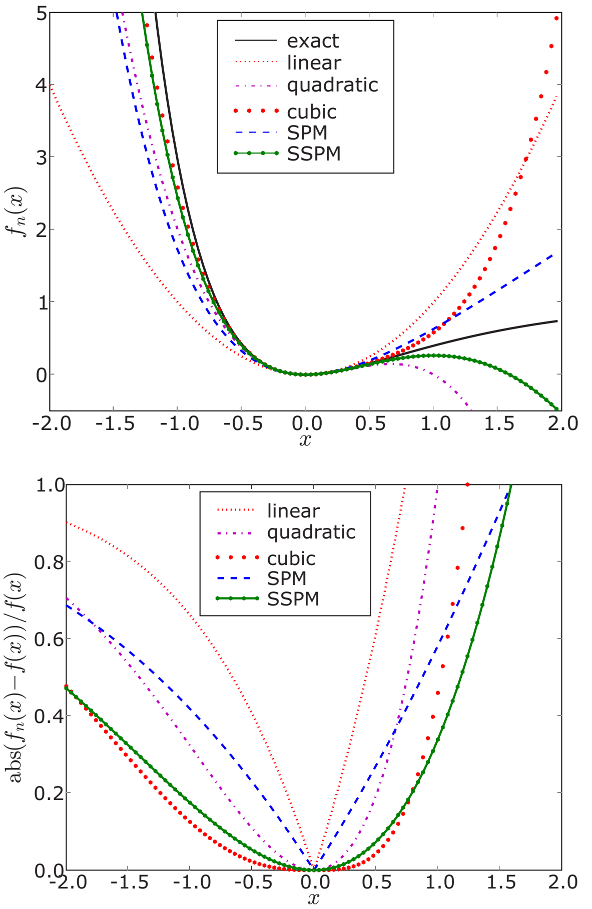

FIG. 2. (Color online) Upper figure: dependence of the effective pair potential between two repulsive colloidal particles on the interaction strength parameter $x=\beta V_0$: exact result versus the SPM and SSPM, and perturbations at various orders. Lower figure: relative errors $|f_n(x)-f(x)|/f(x)$.

the nth-order response estimate to f, and hence to the pair potential, by a simple Taylor expansion of $f(x)$, keeping terms up to $(n+1)$th order in $x=\beta V_0$—i.e.,

$$f(x) = x^2 - x^3 + \frac{7}{12}x^4 + \cdots .$$

Expansions up to cubic order are shown in Fig. 2, together with the SPM result [Eq. (11)]

$$f_{SPM}(x) = (1 - e^{-x})x = x^2 - \frac{x^3}{2} + \frac{x^4}{6} + \cdots$$

and the SSPM result [Eq. (12)]

$$f_{SSPM}(x) = 2\left(x(1 - e^{-x}) - \frac{x^2}{2}\right) = x^2 - x^3 + \frac{x^4}{3} + \cdots .$$

Negative values of x are included in Fig. 2 for illustrative purposes. One can again observe that because of the additional terms it includes, the SSPM is more accurate than linear and quadratic response for all V_0 and more accurate than the SPM for $x<1.59$. Cubic response, on the other hand, is closer to the exact result than the SSPM for $-1.93<x<0.78$, which is expected since the SSPM does not include all cubic terms. For larger $|x|$, though, the higher-order terms play a more important role and the SSPM is more accurate than cubic response.

This example is also instructive in that it allows us to study directly the convergence of response theory. Note that for $V_0<0$ the convergence is monotonous, while for $V_0>0$ there is a more complex, alternating approach to the exact result. This can be traced back to the fact that changing the overall sign of the perturbing potential results in changing the sign of odd orders in response, without affecting the even orders. Thus, if a potential exhibits monotonous convergence, its additive inverse exhibits alternating convergence. We might therefore expect, for example, that effective interactions with protons and antiprotons in an electron gas will have completely different convergence behaviors. If this classical example is to be representative, protons would then exhibit uniform convergence, while antiprotons should exhibit alternating convergence.

Note, finally, that in the problem at hand, response theory converges even for arbitrarily large V_0 and $D+\delta$. Since for repulsive spheres the functions $f(\beta V)$ approaches a constant value exponentially, it is even possible, in this case, to obtain a quantitative value for the limit $V_0\to\infty$ by keeping only a finite number of perturbation terms.

C. The hydrogen molecule and connections with the Heitler-London approach

We move on to the more realistic system composed of two initially bound proton-electron systems immersed in a uniform, neutral, and *interacting* jellium[30–32] at a temperature much lower than the Fermi temperature. This hydrogen-in-jellium problem can be linked to real systems in two ways. First, it can be seen as a first step in a formal expansion including three- and many-center terms which, if carried to all orders, should yield the exact total energy of the system, within the adiabatic approximation. In can also be used within an effective-medium approach[33] in an attempt to take into account the many-ion effects in an approximate way. In both cases the pair potentials can be used to derive phonon spectra. In particular, the pair potentials obtained from quadratic response were used to predict the infrared and Raman vibron frequencies of the hydrogen solid.[17]

To establish a basis of comparison, we first obtain an estimate of the importance of nonlinear corrections to the one-atom density, $\delta\rho_a$, using the *ab initio* program VASP.[34,35] This allows us to estimate the effect on the pair potentials of the higher-order terms in the determination of $\delta\rho_a$.

To obtain this, we used a cubic cell of side $13.5a_0$ containing 74 electrons (for $r_s=2$), together with a $6\times6\times6k$-space grid and a standard projector augmented wave (PAW) pseudopotential for hydrogen[36,37] with cutoffs up to 450 eV. The generalized gradient approximation (GGA) to the exchange-correlation potential, as parametrized by Perdew and Wang,[38] was used, together with the Methfessel-Paxton smearing,[39] with a smearing temperature of $\sigma=0.2$ eV. Since it was shown[18] that the proton-proton pair potential does not depend strongly on the choice of a

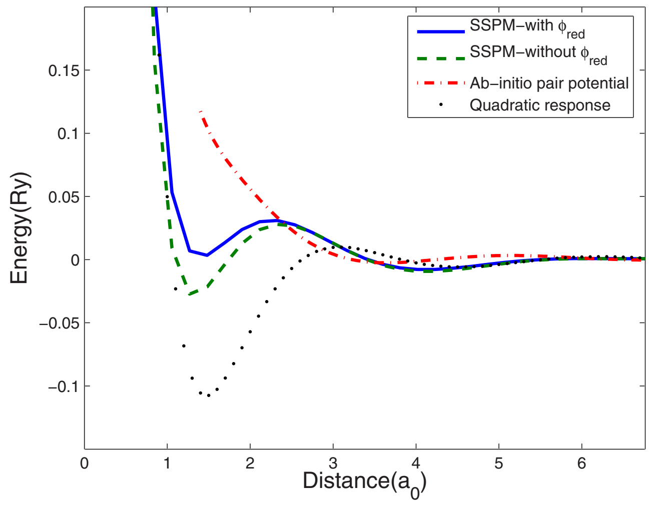

FIG. 3. (Color online) Comparison of the SSPM results with and without contributions from Eq. (13) to quadratic response and *ab initio* results [from Bonev and Ashcroft (Ref. 18)] for proton-proton pair potentials at r_s=2.

pseudopotential, cutoff energy, and exchange-correlation functional, our choice of parameters should yield sufficient precision for our purposes, even considering possible short-range distortions due to core overlap.

The SSPM pair potentials thus obtained are shown in Fig. 3 and are compared with the VASP results for the pair potentials from Bonev and Ashcroft,[18] the quadratic response results, and the SSPM pair potentials corrected by the inclusion of Eq. (13) to lowest order in the perturbing potential.

To obtain the latter, we start with Eq. (13) and use

$$\delta\rho_a^{NL}(\mathbf{k}) \simeq \frac{1}{\Omega}\sum_{\mathbf{k}',\mathbf{k}''}\chi^{(2)}(-\mathbf{k},\mathbf{k}',\mathbf{k}'')V_{ext}(\mathbf{k}')V_{ext}(\mathbf{k}'').$$

This corresponds to the energy diagram shown as Fig. 5(a), below.

We use the second-order noninteracting response function of the homogeneous electron gas, $\chi_0^{(2)}(\mathbf{k},\mathbf{k}',\mathbf{k}')$, in the form given by Milchev and Pickenhain.[10] The interacting response function is then written as

$$\chi^{(2)}(\mathbf{k},\mathbf{k}',\mathbf{k}') = \frac{\chi_0^{(2)}(\mathbf{k},\mathbf{k}',\mathbf{k}')}{\epsilon(\mathbf{k})\epsilon(\mathbf{k}')\epsilon(\mathbf{k}'')},$$

which corresponds to the random phase approximation. This approximation is expected to improve as the density is increased (see, e.g., Pines and Nozières[22]) and should be sufficient to give us information on the general behavior of the potential. Finally we choose the Vashishta-Singwi form[40] for the local field correction $G(\mathbf{k})$.

Under these assumptions we obtain the contribution to the pair potentials displayed in Figs. 3 and 4.

We see that the inclusion of the potential ϕ_{red} from Eq. (13), and therefore of the density-density interaction $\tilde{v}(q) = \epsilon(q)[v_c(q)+\mu_1(q)]$, leads to a contribution to the pair potential that is repulsive at typical proton-proton separation. This behavior largely arises from the Coulomb repulsion term v_c. This contribution therefore explains part, but not all, of the discrepancy observed between the pair potentials obtained from quadratic response[17] and *ab initio* methods.[18] In particular, all perturbation-based methods yield a local minimum around $R=1.4a_0$, whereas no such minimum is observed in the VASP pair potential at the considered density; such a minimum appears for VASP pair potentials only at lower densities, corresponding to $r_s \gtrsim 3$ (see Bonev and Ashcroft[18]). The consequences of the disappearance of this local minimum at higher density for the stability of the hydrogen molecule (or crystal) has also been discussed in Nagao *et al.*[17] and Díez Muiño and Salin.[31]

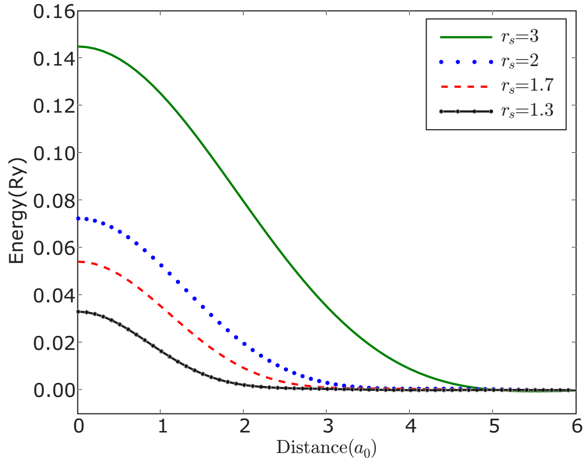

FIG. 4. (Color online) Contribution of the diagram from Fig. 5(a) to the proton-proton pair potential for various values of r_s.

Note that for each diagram of the form shown in Fig. 5(a) there are two similar diagrams of the form shown in Fig. 5(b) which are not reducible and hence not contained in Eq. (13). In the limiting case where the interparticle distance tends to zero, though, diagrams 5(a) and 5(b) should provide the same contribution. Therefore diagrams of the form 5(b) should also have an overall repulsive behavior, contributing to further reduce the discrepancy between perturbative and VASP results.

Note also that if we consider separately the contributions of $\tilde{v}_c(q)=\epsilon(q)v_c(q)$ and $\tilde{\mu}_1=\epsilon(q)\mu_1(q)$, we find that the contribution of $\tilde{\mu}_1$ is mostly attractive, as can be seen in Fig. 6 for r_s=2. We also observe that terms arising from Eq. (13) exhibit very weak Friedel oscillations. This distinguishes these terms from the other contributions calculated here or *ab initio* pair potentials[18] (compare, e.g., Figs. 3 and 4), and

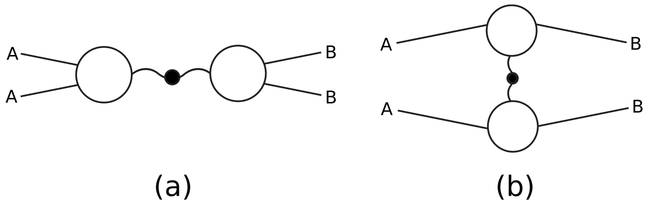

FIG. 5. (a) Lowest-order diagram contributing to the interaction (13). (b) Nonreducible diagram equal to diagram (a) in the limit $R_{ab}\rightarrow 0$, for identical ions, here protons (diagrammatic conventions are explained in Appendix A and Fig. 7).

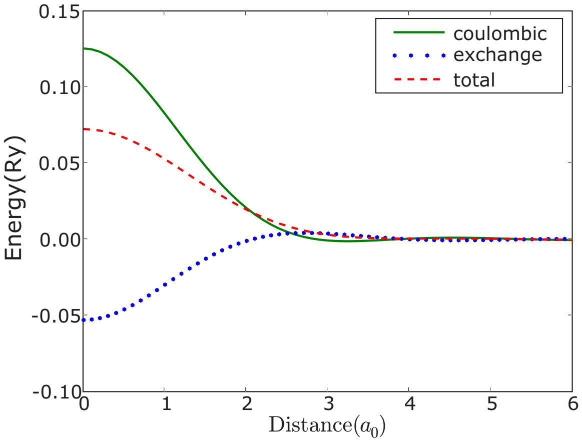

FIG. 6. (Color online) Contributions of the Coulombic and exchange parts to the effective electron-electron potential $\tilde{v}$, for $r_s=2$.

we conjecture that this arises from the reducibility of the energy diagram.

We draw the reader's attention to the close similarity of the pair potential of Eq. (15) with corresponding terms in the Heitler-London (HL) picture of the isolated hydrogen molecule. We can identify in both methods (i) the ion-ion repulsions, (ii) the attractive interactions between ion b (a, respectively) with the density induced by a (b, respectively), (iii) the Coulombic repulsion between the one-atom electronic densities, and (iv) an attractive exchange contribution from the electrons. The fourth term in Eq. (15), which has no equivalent in the HL picture, goes to zero in the low-density, free-molecule case. It is interesting that two such different approaches, one being variational in essence and the other one perturbational, yield such similar results.

Some features of the HL pictures cannot be observed in the SSPM, though, because of the nonzero average electronic density considered in the SSPM. For example, while the pair potential between protons immersed in spin-polarized or spin-unpolarized electrons differed only by the exchange term in HL, this is no longer the case in the SSPM approach. The densities $\delta\rho_i$ induced by single protons are indeed quite different for spin-polarized and spin-unpolarized electrons.

V. CONCLUSION

To obtain effective interactions between particles immersed in a well-understood system, such as ions immersed in a uniform jellium, the traditional perturbation approach treats all immersed particles as a single perturbation. One finds the free energy of the perturbed system as a function of the total perturbation potential. The total potential is then separated in the sum of its constituents, which allows a natural separation of the effective potential in pair-, triplet-, and many-body potentials.

Here we have discussed two alternative approaches. In the first approach, we start by immersing a single particle in the well-understood system and then calculate the response functions of the new, but perturbed system. Since these response functions are directly related to the electronic density or density-density correlation functions, they can be obtained by a variety of techniques, including perturbation theory, simulations, and density functional theory and even deduced from experiment. The remaining particles are then treated as a further perturbation of this already perturbed system.

Such a two-step process is ideal when only one perturbation is strong,[24] but it is intrinsically asymmetrical and not ideal when both perturbations are large enough to induce nonlinear effects. We have suggested a way to improve and symmetrize this procedure which allows one to treat an increased number of perturbation terms with little additional effort. More specifically, by using results of the asymmetrical approach that are exact to linear order in the perturbation potential, it is possible to construct a symmetrized result exact to quadratic order and including additional higher-order terms as well. We applied this method to two simple noninteracting test systems and found that it improves upon standard linear and quadratic response, as expected.

More importantly, it was shown that this simple method could be naturally refined by the inclusion of higher-order terms describing, in particular, electron-electron interactions. These higher-order terms also have intuitive physical meaning, and we used this to argue that the standard termination of the perturbation series at a given order is not the best strategy. The inclusion of the higher-order terms was indeed shown to improve considerably the agreement between the perturbation and density functional theory approaches in the problem of proton-proton pair potentials.

Even though we considered here effective interactions between identical particles only, the SSP method is particularly well suited to the description of systems with multiple (say, N) types of particles. It indeed reduces the computational difficulty from the determination of $N^2/2$ pair potentials to that of finding N (typically symmetric) induced densities, from which the pair potentials can be obtained in a straightforward manner. It can also be generalized to many-center interactions and to magnetic perturbations (see Appendix B).

Finally, a striking similarity is found between terms in the pair potentials arising from this approach and from the Heitler-London variational approach for diatomic molecules, leading to a possible natural generalization of the Heitler-London approach to metallic systems. This similarity could be explored further by comparing the pair potential for a pair of atoms in a jellium, as derived here, to a pair of atoms in a Wigner-Seitz spherical cell ensuring the same average density, which could be treated within a Heitler-London-like approach.

A more detailed comparison of the SSPM and *ab initio* pair potentials for hydrogen and other materials, especially at densities higher than those considered here, would be a logical next step to this work, as would be a more detailed treatment of the many-body interactions, both from the *ab initio* and SSPM perspectives.

ACKNOWLEDGMENTS

We would like to thank Bruno Rousseau for many enlightening discussions and also Stanimir Bonev, Ji Feng, James

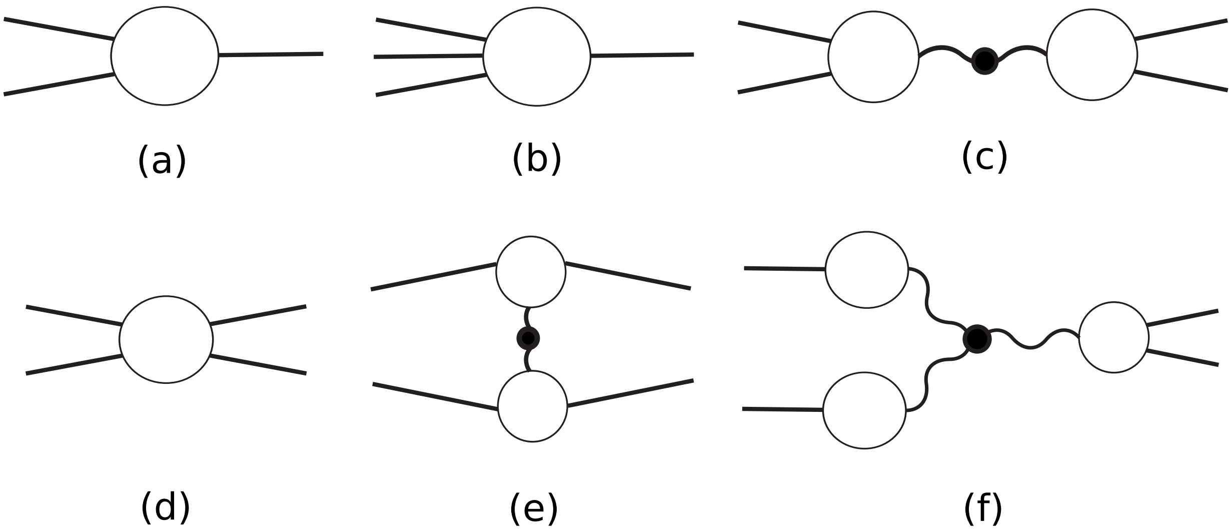

FIG. 7. Some typical diagrams from the free energy expansion contributing to the pair potential. Loops with $n+1$ legs represent response function of order n. The correlation function $c_0^{(n)}$ is represented by a solid circle surrounded by $n+1$ wavy lines and the external potential by solid lines. Diagram (a) is a quadratic response contribution. Diagrams (b) and (c) represent some third-order contributions taken into account by Eqs. (12) and (13), respectively. Diagrams (d), (e), and (f) are examples of cubic-response contributions which are *not* taken into account in the approach presented here.

Porter, and David Roundy. This work was supported by NSF Grant No. DMR-0601461 and by a PGS research grant from NSERC.

APPENDIX A: DERIVATION OF EQ. (13)

We first use the Hohenberg-Kohn-Sham approach[41,42] (and the finite-temperature extension due to Mermin[43]) to write the induced density in terms of the response functions of a noninteracting system in a modified external potential (see, e.g., Lundqvist and March[44]). We write the density as

$$\delta\rho(\mathbf{k}) = \sum_{\mathbf{k}'} \chi_0^{(1)}(-\mathbf{k},\mathbf{k}')\Gamma(\mathbf{k}') + \frac{1}{\Omega}\sum_{\mathbf{k}',\mathbf{k}''} \chi_0^{(2)}(-\mathbf{k},\mathbf{k}',\mathbf{k}'')\Gamma(\mathbf{k}')\Gamma(\mathbf{k}'') + \cdots, \tag{A1}$$

where $\chi_0^{(n)}$ are the response functions of the noninteracting system and Γ is the *effective* perturbation potential. We write Γ as

$$\Gamma(\mathbf{k},\lambda) = \lambda V(\mathbf{k}) + c(\mathbf{k},[\rho]) - c(\mathbf{k},[\rho_0]), \tag{A2}$$

where $\beta c(\mathbf{k},[\rho])$ is the first-order direct correlation function.

The parameter λ is introduced to keep track of the order of the expansion. For example, we can write

$$\Gamma(\mathbf{k}) = \lambda\Gamma^{(1)}(\mathbf{k}) + \lambda^2\Gamma^{(2)}(\mathbf{k}) + \cdots . \tag{A3}$$

The variation $\delta c(\mathbf{k},[\rho]) = c(\mathbf{k},[\rho]) - c(\mathbf{k},[\rho_0])$ can in turn be written as a functional expansion:

$$\delta c(\mathbf{k}) = \sum_{\mathbf{k}'} c_0^{(1)}(-\mathbf{k},\mathbf{k}')\,\delta\rho(\mathbf{k}') + \frac{1}{\Omega}\sum_{\mathbf{k}',\mathbf{k}''} c_0^{(2)}(-\mathbf{k},\mathbf{k}',\mathbf{k}'')\,\delta\rho(\mathbf{k}')\,\delta\rho(\mathbf{k}'') + \cdots . \tag{A4}$$

Note that here $\beta c_0^{(i)}$ is the $(i+1)$th direct correlation function of the unperturbed system. This slightly unusual notation is chosen to emphasize the similarity between Eqs. (A1) and (A4).

Finally the induced density can also be expressed in powers of the external potential:

$$\delta\rho(\mathbf{k}) = \lambda\,\delta\rho^{(1)}(\mathbf{k}) + \lambda^2\,\delta\rho^{(2)}(\mathbf{k}) + \cdots . \tag{A5}$$

The variation in the free energy is obtained as before through Eq. (8), which we now write as

$$\Delta F = \frac{1}{\Omega}\sum_{\mathbf{k},n} \frac{\rho^{(n)}(\mathbf{k})V_{ext}(-\mathbf{k})}{n+1} = \Delta F_1 + \frac{1}{\Omega}\sum_{\mathbf{k},n} \frac{\delta\rho^{(n)}(\mathbf{k})V_{ext}(-\mathbf{k})}{n+1}, \tag{A6}$$

where ΔF_1 does not depend on the relative positions of the perturbation sources and will therefore not contribute to the pair potentials.

Using Eqs. (A1), (A2), and (A4), we can represent each term in Eq. (A6) by a diagram using three types of building blocks: namely, $\chi_0^{(n)}$ and $c_0^{(n)}$ for $n \geq 1$, and V_{ext}. A few examples are shown in Fig. 7.

Each V_{ext} is connected to a single $\chi_0^{(n)}$. Each $c_0^{(n)}$ is connected to $n+1$ different $\chi_0^{(n)}$. Each $\chi_0^{(n)}$ is connected to $n+1$ blocks that can be either V_{ext}, or a $c_0^{(n)}$. Conversely, every treelike diagram obeying these rules corresponds to a term in

FIG. 8. Diagrammatic expansion for the dressed $\tilde{c}_0^{(1)}$ in terms of the bare $c_0^{(1)}$ and linear response functions.

Eq. (A6). Note that since $\delta\rho(\mathbf{q})$ obeys the same rules, it can be represented by the same diagrams, with only one V_{ext} removed.

We call reducible those diagrams in Eq. (A6) that can be separated, by the cutting of a single $c_0^{(1)}$ line, into two diagrams that depend exclusively on V_a or on V_b, respectively, and that are linear in neither V_a nor V_b. On Fig. 7, diagram (c) is reducible, while the others are not.

We want to show that the set of such diagrams is equivalent to those described by Eq. (13). First we will show that there is a one-to-one correspondence between reducible diagrams in Eq. (A6) and diagrams in Eq. (13). Then we will show that the prefactors also agree.

1. Diagrammatic equivalence

Consider a reducible diagram D contributing to the pair potential. Then consider the set S of all diagrams that are different from D only by the number of separating interaction lines. The separating interaction lines can only be connected by $\chi_0^{(1)}$ loops. By summing over the different numbers of $\chi_0^{(1)}$ loops and the momenta associated with these loops, we can therefore obtain a dressed propagator in terms of a dielectric function,

$$\tilde{c}_0^{(1)}(\mathbf{k},\mathbf{k}') = \frac{c_0^{(1)}(\mathbf{k},\mathbf{k}')}{\epsilon(\mathbf{k},\mathbf{k}')} \tag{A7}$$

which takes a simple form in the diagrammatic language (see Fig. 8).

All diagrams in S are therefore included in $\Sigma_{\{\mathbf{k}\}}D_1(\{\mathbf{k}\})/\epsilon(\mathbf{k}_i,\mathbf{k}_j)$ where $D_1(\{\mathbf{k}\})$ is the value, *before* the summation over the momenta $\{\mathbf{k}\}$, of the diagram in S with a single separating $c_0^{(1)}$ propagator. $\mathbf{k}_i$ and $\mathbf{k}_j$ are the momenta of the separating propagator.

Since we can construct diagrams contributing to $\delta\rho(\mathbf{k})$ with the same building blocks and the same construction rules as for diagrams contributing to the pair potential, it is easy to find an expression involving only $\delta\rho_i$ and $c_0^{(1)}$ that includes all reducible diagrams contributing to the pair potential. An example of such an expression is

$$\frac{1}{\Omega}\sum_{\mathbf{k},\mathbf{k}'}\delta\rho_a^{NL}(\mathbf{k},\mathbf{R}_a)c_0^{(1)}(\mathbf{k},\mathbf{k}')\delta\rho_b^{NL}(\mathbf{k}',\mathbf{R}_b).$$

Since both $\delta\rho_a(\mathbf{k})$ and $\delta\rho_b(\mathbf{k})$ have an arbitrary number of $\chi_0^{(1)}$ loops on the leg with momenta $\mathbf{k}$, though, this expression amounts to screening the $c_0^{(1)}$ interaction twice. To take care of this, we can write instead

$$\phi_{red}(\mathbf{R}_a,\mathbf{R}_b) = \frac{1}{\Omega}\sum_{\mathbf{k},\mathbf{k}'}\delta\rho_a^{NLU}(\mathbf{k},\mathbf{R}_a)\frac{c_0^{(1)}(\mathbf{k},\mathbf{k}')}{\epsilon(\mathbf{k},\mathbf{k}')}\delta\rho_b^{NLU}(\mathbf{k}',\mathbf{R}_b), \tag{A8}$$

where $\delta\rho_a^{NLU}(\mathbf{k},\mathbf{R}_a)$ is defined as the sum of all diagrams in $\delta\rho_a^{NL}(\mathbf{k},\mathbf{R}_a)$ without $\chi^{(1)}$ loops on the leg with the $\mathbf{k}$ momentum (U stands for unscreened). To each reducible diagram contributing to the pair potential corresponds a diagram in Eq. (A8) and vice-versa.

For homogeneous systems, we have

$$\chi^{(1)}(\mathbf{k},\mathbf{k}') = \chi^{(1)}(k')\delta_{\mathbf{k},-\mathbf{k}'},$$

$$c_0^{(1)}(\mathbf{k},\mathbf{k}') = c_0^{(1)}(k')\delta_{\mathbf{k},-\mathbf{k}'},$$

$$\frac{1}{\epsilon(\mathbf{k},\mathbf{k}')} = \frac{1}{\epsilon(k)} = \sum_i [c_0^{(1)}(k)\chi_0^{(1)}(k)]^i = \frac{1}{1-c_0^{(1)}(k)\chi_0^{(1)}(k)},$$

and

$$\delta\rho_{a,b}(\mathbf{k},\mathbf{R}_{a,b}) = \rho_{a,b}(\mathbf{k})e^{i\mathbf{k}\cdot\mathbf{R}_{a,b}},$$

so that Eq. (A8) simplifies to

$$\phi_{red}(\mathbf{R}_{ab}) = \frac{1}{\Omega}\sum_{\mathbf{k}}\delta\rho_a^{NL}(\mathbf{k})c_0^{(1)}(k)\epsilon(k)\delta\rho_b^{NL}(-\mathbf{k})e^{i\mathbf{k}\cdot\mathbf{R}_{ab}},$$

which is precisely Eq. (13); we have shown that Eq. (13) contains exactly the reducible diagrams from Eq. (A6). Now we need to show that the prefactors of these diagrams also agree.

2. Prefactors and symmetries

A diagram D is said to possess a symmetry of order m if it is possible to cut m legs from a given χ_0 or c_0 and obtain m identical cut-down parts. Each such symmetry contributes a factor $1/m!$ to the total prefactor of the diagram, as compared to an equivalent asymmetrical diagram.

In order to obtain this "equivalent asymmetrical diagram," we replace V_{ext} by $\tilde{V}_{ext}=\Sigma_{j=1}^{n+1}v_j$ in the original problem, where $n+1$ is the number of external legs of diagram D. We then consider the diagram $\tilde{D}$ that is identical to D, apart from its external legs which are all connected to different v_j. By construction, diagram $\tilde{D}$ can have no symmetry.

Contributions to diagram $\tilde{D}$ can be obtained, in Eq. (A6), by replacing V_{ext} by any of the v_j and by calculating the prefactor P_j of the density diagram obtained by removing v_j from $\tilde{D}$. The prefactor $P_{\tilde{D}}$ of $\tilde{D}$ is therefore

$$P_{\tilde{D}} = \frac{1}{n+1}\sum_{\substack{j:\,\text{external}\\ \text{leg}}} P_j, \tag{A9}$$

Since there is no symmetry in the diagram, it is relatively straightforward to find its prefactor: each $\chi_0^{(i)}$ or $c_0^{(i)}$ contributes $i!$ to the global prefactor. Therefore all P_j are equal, the $(n+1)$ factors cancel out, and we simply get $P_{\tilde{D}}=P_j$. By a similar argument, we obtain

$$P_{\tilde{D}} = P_j = P_{\tilde{D}_a} P_{\tilde{D}_b},$$

where $\tilde{D}_a$ and $\tilde{D}_b$ are the separated diagrams. Asymmetric reducible diagrams therefore have the same prefactor in Eqs. (A6) and (13).

This result can be extended to symmetrical diagrams in a straightforward manner: if the two identical diagrams obtained by cutting two legs from a given χ or μ in a symmetrical reducible diagram, they cannot contain the separating interaction line. Therefore all symmetries are contained within the separated diagrams. Since each symmetry contributes a factor $1/m!$ to the global prefactor, m being the number of identical branches involved in this symmetry, the symmetry contributions to Eqs. (13) and (A6) are the same.

We have therefore derived the result that there is a one-to-one correspondence between reducible diagrams contributing to the pair potential [in Eq. (A6)] and diagrams contained in Eq. (13). Since the prefactors of these diagrams in each expression also agree, Eq. (13) allows the calculation of the pair potential associated with all reducible diagrams.

APPENDIX B: GENERALIZATIONS

In this appendix we discuss two possible generalizations of the methods introduced above: namely, the case of magnetic perturbations and that of many-center interactions.

1. Magnetic perturbations and the RKKY interaction

The interaction between magnetic perturbations (e.g., nuclear spins or magnetic impurity atoms) and an electron gas can be modeled by the Hamiltonian[45]

$$H_{int,\lambda} = \lambda J \sum_{i,j} f(\mathbf{r}_i - \mathbf{R}_j)\mathbf{S}^j \cdot \vec{\sigma}^i,$$

where $\mathbf{r}_i$ and $\vec{\sigma}^i$ are the position and spin operators for electron i, while $\mathbf{R}_j$ and $\mathbf{S}^j$ are the position and spin of the jth magnetic perturbation source.

The Hellman-Feynman theorem reads

$$F_1 - F_0 = \int_0^1 d\lambda \langle H_{int,1}\rangle_\lambda = J\int_0^1 d\lambda \sum_j \int d\mathbf{r} f(\mathbf{r}-\mathbf{R}_j)\mathbf{S}^i \cdot \mathbf{m}(\mathbf{r})_\lambda, \tag{B1}$$

where the local magnetization $\mathbf{m}$ is given by

$$\mathbf{m}(\mathbf{r})_\lambda = \left\langle \sum_i \delta(\mathbf{r}_i - \mathbf{r})\vec{\sigma}^i \right\rangle_\lambda .$$

By analogy with the induced density case, we can describe the perturbation using

$$V_j(\mathbf{r}) = J\sum_i f(\mathbf{r}-\mathbf{R}_i)S_j^i.$$

Assuming a nonmagnetic unperturbed state,

$$m_i(\mathbf{r})_\lambda = \int d\mathbf{r}\, \chi_{ij}(\mathbf{r},\mathbf{r}')\lambda V_j(\mathbf{r}') + \int d\mathbf{r}' d\mathbf{r}'' \chi^{(2)}_{ijk}(\mathbf{r},\mathbf{r}',\mathbf{r}'')\lambda^2 V_j(\mathbf{r}')V_k(\mathbf{r}'') + \cdots .$$

If we have two magnetic perturbing sources (a and b), we find an effective interaction of the form

$$\phi(\mathbf{R}_a,\mathbf{R}_b,\mathbf{S}^a,\mathbf{S}^b) = \int d\mathbf{r} V^a(\mathbf{r})\cdot \mathbf{m}^b(\mathbf{r},\mathbf{R}_b,\mathbf{S}^b) + \int d\mathbf{r} V^b(\mathbf{r})\cdot \mathbf{m}^a(\mathbf{r},\mathbf{R}_a,\mathbf{S}^a) - \int d\mathbf{r} d\mathbf{r}' \chi_{ij}(\mathbf{r},\mathbf{r}')V_i^a(\mathbf{r})V_j^b(\mathbf{r}'). \tag{B2}$$

Here, as before, V^i describes the perturbation associated with source i and $\mathbf{m}^i(\mathbf{r},\mathbf{R}_i,\mathbf{S}^a)$ is the magnetization induced at $\mathbf{r}$ by the presence of a single perturbation of spin S^i at R_i.

In the particular case of pointlike magnetic perturbations [$f(\mathbf{r})=\delta(\mathbf{r})$], the effective interaction between the magnetic perturbations takes the simple form

$$\phi(\mathbf{R}_a,\mathbf{R}_b,\mathbf{S}^a,\mathbf{S}^b) = JS^a \cdot \mathbf{m}^b(\mathbf{R}_a,\mathbf{R}_b,\mathbf{S}^b) + JS^b \cdot \mathbf{m}^a(\mathbf{R}_b,\mathbf{R}_a,\mathbf{S}^a) - J^2\chi_{ij}(\mathbf{R}_a,\mathbf{R}_b)S_i^a S_j^b. \tag{B3}$$

This expression, which goes beyond quadratic response [but does not include corrections of the form (13)], could be used to improve upon the standard RKKY potential, which takes into account only the linear order in response.[3]

2. Many-center potentials

Since the sources of the perturbations in Eqs. (12) and (13) have not been specified, a straightforward way of treating many-particle interactions in this formalism is to take either or both sources to be an ensemble of particles. This might be especially appropriate for problems involving the diffusion of well-formed molecules. In the hydrogen problem, this could also be used to study the molecule-molecule interactions near or beyond the onset of metallization.

Many-center interactions can be treated in a more symmetric way through conventional response theory (see, e.g., Porter[46]), but also through a SSPM approach. The lowest-order N-body term arises at the level of $(N-1)$th-order response. This term is linear in the potential from all N particles. The next most dominant contributions will be from terms that are nonlinear in the potential arising from one particle and linear in that arising from the remaining $N-1$.

We can directly generalize Eq. (12) to an N-body potential treating all terms linear in $N-1$ particles exactly by writing

$$\phi^{(N)}(\{\mathbf{R}\}) \simeq \frac{1}{(N-1)\Omega}\sum_{j=1}^{N}\sum_{\mathbf{k}} V_j(\mathbf{k})\,\delta\tilde{\rho}_{[j]}(-\mathbf{k})e^{i\mathbf{k}\cdot\mathbf{R}_j} - \frac{1}{(N-1)\Omega^{N-1}}\sum_{\{\mathbf{k}_i\}}\chi^{(N-1)}(\mathbf{k}_1,\ldots,\mathbf{k}_N) \times\prod_{j=1}^{N} V_j(\mathbf{k}_j)e^{i\mathbf{k}_j\cdot\mathbf{R}_j}. \tag{B4}$$

Here $\delta\rho_{[j]}(\mathbf{k})$ is the density induced by all involved particles *except* j and $\delta\tilde{\rho}_{[j]}(\mathbf{k})$ is the component of this density that depends on the position of all $N-1$ particles involved. The latter definition is required simply to avoid double counting the potentials involving less than N particles.

Equation (B4) provides in principle a way to obtain an expression that is exact up to Nth order, requiring only explicit knowledge of the $(N-1)$th-order response function. On the other hand, it requires knowledge of the density induced by N groups of $N-1$ particles, which rapidly becomes more difficult when $N>2$.

---

[1] M. Cohen, V. Heine, and D. Weaire, Solid State Phys. **24** (1970).

[2] J. Hafner, *From Hamiltonians to Phase Diagrams* (Springer-Verlag, New York, 1987).

[3] C. Kittel, *Solid State Physics* (Academic, New York, 1968), p. 1; see also erratum in Appendix A (p. 295).

[4] B. Derjaguin and L. Landau, Acta Physicochim. URSS **14**, 633 (1941).

[5] E. Verwey and J. Overbeek, *Theory of the Stability of Lyophobic Colloids* (Dover, Mineola, NY, 2000).

[6] S. Asakura and F. Oosawa, J. Chem. Phys. **22**, 1255 (1954).

[7] S. Asakura and F. Oosawa, J. Polym. Sci. **33**, 183 (1958).

[8] P. Lloyd and C. Sholl, J. Phys. C **1**, 1620 (1968).

[9] E. Brovman, Y. Kagan, and A. Kholas, Sov. Phys. JETP **34**, 394 (1972).

[10] A. Milchev and R. Pickenhain, Phys. Status Solidi B **79**, 549 (1977); J. Porter, N. W. Ashcroft, and G. V. Chester (unpublished).

[11] J. M. Pitarke, R. H. Ritchie, and P. M. Echenique, Phys. Rev. B **52**, 13883 (1995).

[12] G. Angilella, F. Siringo, and R. Pucci, Eur. Phys. J. B **32**, 323 (2003).

[13] A. Lodder, Phys. Rev. B **74**, 045111 (2006).

[14] S. T. Weir, A. C. Mitchell, and W. J. Nellis, Phys. Rev. Lett. **76**, 1860 (1996).

[15] P. Loubeyre, F. Occelli, and R. LeToullec, Nature (London) **416**, 613 (2002).

[16] A. A. Louis and N. W. Ashcroft, Phys. Rev. Lett. **81**, 4456 (1998).

[17] K. Nagao, S. A. Bonev, A. Bergara, and N. W. Ashcroft, Phys. Rev. Lett. **90**, 035501 (2003).

[18] S. A. Bonev and N. W. Ashcroft, Phys. Rev. B **64**, 224112 (2001).

[19] J. Ziman, *Electrons and Phonons* (Oxford University Press, New York, 2001).

[20] In the case of neutral systems composed of oppositely charged particles, such as metals, care should be taken to define the perturbing and perturbed systems in such a way that thermodynamic functions such as $F_A(\{\mathbf{R}\},T)$ are well defined. This can be achieved by requiring that each physical, charged particle "carries" a uniform compensating charged background filling the whole available volume, ensuring a cancellation of divergent $\mathbf{k}=0$ terms (see also Ref. 46, below). In this case both the perturbed and perturbing systems are neutral and thermodynamically well defined, and in the combined system the compensating backgrounds cancel out, so we recover the physical system. In the case of the electron gas the perturbed system is simply jellium.

[21] It is assumed here that the free energy varies continuously while λ goes from 0 to 1.

[22] D. Pines and P. Nozières, *The Theory of Quantum Liquids I* (Benjamin, New York, 1966), p. 297.

[23] R. Elber, *Recent Developments in Theoretical Studies of Proteins* (World Scientific, Singapore, 1996), p. 43.

[24] Z. D. Popovic, M. J. Stott, J. P. Carbotte, and G. R. Piercy, Phys. Rev. B **13**, 590 (1976).

[25] Y. Yafet, Phys. Rev. B **36**, 3948 (1987).

[26] G. F. Giuliani, G. Vignale, and T. Datta, Phys. Rev. B **72**, 033411 (2005).

[27] *Handbook of Mathematical Functions*, edited by M. Abramowitz and I. Stegun (Dover, New York, 1965).

[28] A. A. Louis, Ph.D. thesis, Cornell University, 1998.

[29] A. Galindo, I. Nagy, R. Díez Muiño, and P. M. Echenique, Phys. Rev. B **72**, 125113 (2005).

[30] J. K. Nørskov, Phys. Rev. B **20**, 446 (1979).

[31] R. Diez Muiño and A. Salin, Phys. Rev. B **60**, 2074 (1999).

[32] O. B. Christensen, P. D. Ditlevsen, K. W. Jacobsen, P. Stoltze, O. H. Nielsen, and J. K. Nørskov, Phys. Rev. B **40**, 1993 (1989).

[33] K. W. Jacobsen, J. K. Nørskov, and M. J. Puska, Phys. Rev. B **35**, 7423 (1987).

[34] G. Kresse and J. Furthmüller, Phys. Rev. B **54**, 11169 (1996).

[35] G. Kresse and J. Furthmuller, Comput. Mater. Sci. **6**, 15 (1996).

[36] G. Kresse and D. Joubert, Phys. Rev. B **59**, 1758 (1999).

[37] P. E. Blochl, Phys. Rev. B **50**, 17953 (1994).

[38] J. Perdew, in *Electronic Structure of Solids* (Akademie-Verlag, Berlin, 1991), pp. 11–20.

[39] M. Methfessel and A. T. Paxton, Phys. Rev. B **40**, 3616 (1989).

[40] P. Vashishta and K. S. Singwi, Phys. Rev. B **6**, 875 (1972).

[41] P. Hohenberg and W. Kohn, Phys. Rev. **136**, B864 (1964).

[42] W. Kohn and L. Sham, Phys. Rev. **140**, A1133 (1965).

[43] N. Mermin, Phys. Rev. **137**, A1441 (1965).

[44] S. Lundqvist and N. March, *Theory of the Inhomogeneous Electron Gas* (Plenum Press, New York, 1983), p. 124.

[45] A. Hewson, *The Kondo Problem to Heavy Fermions* (Cambridge University Press, Cambridge, England, 1997).

[46] J. A. Porter, Ph.D. thesis, Cornell University, 2001.